2007 IEEE International Conference on
Robotics and Automation
Roma, Italy, 10-14 April 2007

Minimum-norm Solution for the Actuator Forces in Cable-based Parallel Manipulators based on Convex Optimization

Mahir Hassan, and Amir Khajepour

Abstract— **Cable-based Parallel Manipulators (CPM) are light-weight manipulators that can reach high accelerations. The difference between the design of CPM and that of rigid-link parallel manipulators is that cables can only perform while under tension. Redundant limbs, such as extra cables, springs, or cylinders, can be used for applying forces on the mobile platform to generate cable tensions resulting in a redundantly actuated manipulator. To operate this manipulator, the actuator-force distribution amongst the cables and the redundant limbs needs to be determined. Actuator-force optimization techniques developed for rigid-link manipulators are unsuitable for CPM. In this study, a numerical procedure based on convex analysis and optimization is presented to calculate the minimum-norm solution that minimizes the 2-norm of actuator forces. The procedure is based on convex optimization that utilizes the *Dykstra's* alternating projection algorithm to reach to the optimum solution. This numerical method is successfully applied to 3- and 6-degree-of-freedom (DOF) spatial CPMs to determine the optimum actuator forces for a given external load. This study addresses the static analysis in cable-based parallel manipulators in the language of convex analysis.**

I. Introduction

Parallel manipulators consist of a number of branches acting in-parallel on a mobile platform. In cable-based parallel manipulators (CPM), where branches consist of cables instead of rigid links, high accelerations can be achieved due to the reduced mass of the branches enabling CPM to perform ultra-high-speed operations. In CPM, cables should be in tension and that can be achieved by redundant actuation, in which extra loading is applied to the mobile platform. This loading can be obtained from a redundant cable [1],[2] or from another force-applying element such as a spring [3] or a pneumatic cylinder [4]. Since early 1990's, a number of researchers showed interest in studying CPM and several designs were presented in the literature, such as NIST Robocrane [5], Falcon-7 [6], WARP [7], and WiRo [8]. Behzadipour and Khajepour [4] developed a 3-degree-of-freedom (3-DOF) translational cable-based manipulator, DeltaBot, in which cable tensions are maintained by a pneumatic cylinder applying a redundant force to the mobile platform. Russell [3] used a spring to keep the tension of the cables in a robot system designed for small-scale grasping tasks in tension. Mroz and Notash [9] developed a prototype of a hybrid cable-based robot consisting of cables providing actuation and a rigid-link arm providing the constraints required to generate the desired motion at the mobile platform. One of the main issues in the kinematics of CPM is achieving static equilibrium against external loading considering that cables cannot be under compression. Roberts et al. [10] used the null space of the Jacobian matrix to analyze the static equilibrium of CPM at certain configurations. Stump and Kumar [11] used tools from convex analysis and linear algebra to determine whether a CPM is fully constrained at a certain configuration and to calculate its workspace boundaries. Hassan and Khajepour [12] presented a methodology to determine the connection positions of the redundant limb in redundantly-actuated cable-based parallel manipulators.

Because CPM are redundant systems that has more actuators than the task dimensions, infinitely many solutions for the distribution of cable tensions can be obtained for a given external load. One of the issues in the operation of CPM that has not yet received enough attention by researchers is resolving the actuation redundancy and determining the optimum cable forces distribution. Fang et al. [13] presented an analytical method to optimize cable tension distribution in CPM based on minimizing the sum in of cable tensions at every pose. Their method, however, is not applicable to CPM with more than one redundant cable. Determining the optimal cable tension distribution is essential for the efficient control and operation of CPM. This article presents a numerical approach based on convex analysis and optimization to determine the optimum the actuator-force distribution for a given external load based on minimizing the 2-norm of the actuator forces.

II. Background on Convex Analysis and Optimization

To introduce the terms that will be used in this article, this section presents a brief background on convex analysis and optimization based on [14].

A set $\mathcal{S}$ is convex if and only if for all points $\mathbf{y}, \mathbf{x} \in \mathcal{S}$,

$$\mu \mathbf{y} + (1-\mu)\mathbf{x} \in \mathcal{S} \quad (0 \le \mu \le 1) \tag{1}$$

Basically, this definition indicates that for any two points belonging to a convex set, all the points in the line segment that joins the two points also belong to that convex set. The

Mahir Hassan (corresponding author) is a postdoctoral fellow in the Department of Mechanical Engineering, University of Waterloo, Waterloo, Ontario, N2L 3G1, Canada, phone: (519) 888-4567 ×37555; fax: (416) 535-6860; e-mail: m3hassan@uwaterloo.ca.

Amir Khajepour is a professor in the Department of Mechanical Engineering, University of Waterloo, Waterloo, Ontario, N2L 3G1, Canada, e-mail: akhajepour@uwaterloo.ca.

set formed by the intersection of any two convex sets is convex. An open convex set that has no boundaries is called an affine set, which is basically a subset that is a translation of a subspace. A subspace must include the Origin while this is not the case with an affine set. A set $\mathcal{F}$ is affine if and only if for all points $\mathbf{y}, \mathbf{x} \in \mathcal{F}$,

$$\rho\,\mathbf{y} + (1-\rho)\,\mathbf{x} \in \mathcal{F} \qquad (\rho \in \mathrm{R}) \tag{2}$$

In other words, for any two distinct points in $\mathcal{F}$, all the points in the line passing through these two points also belong to $\mathcal{F}$.

Another type of convex set that will often be used in this article is the orthant, which is a closed convex set that is the higher-dimensional generalization of a quadrant from the classical Cartesian partition of R^2 (see Fig. 1). Common examples of orthants are non-negative and non-positive orthants, R^n_+ and R^n_-, respectively. Non-negative orthant R^n_+ is expressed as:

$$\mathrm{R}^n_+ \equiv \left\{ \mathbf{x} \in \mathrm{R}^n \,\middle|\, x_i \geq 0 \;\; \forall i \right\} \qquad (i = 1, \ldots, n) \tag{3}$$

If a closed convex set $\mathcal{S}$ belongs to a subspace $\mathcal{M}$ in R^n, (i.e., $\mathcal{S} \subset \mathcal{M} \subset \mathrm{R}^n$), for every $\mathbf{x} \in \mathrm{R}^n$, there exists a unique projection of $\mathbf{x}$ onto the convex set $\mathcal{S}$, denoted here as $proj_{\mathcal{S}}(\mathbf{x})$, such that the Euclidean distance between $\mathbf{x}$ and $proj_{\mathcal{S}}(\mathbf{x})$ is minimized. The unique minimum-Euclidean-distance projection of $\mathbf{x}$ onto convex set $\mathcal{S}$ can be determined by first projecting $\mathbf{x}$ orthogonally onto subspace $\mathcal{M}$ and then projecting the result onto convex set $\mathcal{S}$, as seen in Fig. 2. This projection can be expressed as:

$$proj_{\mathcal{S}}(\mathbf{x}) = proj_{\mathcal{S}}\left(proj_{\mathcal{M}}(\mathbf{x}) \right) \tag{4}$$

Due to the fact that orthants are self dual, the minimum-

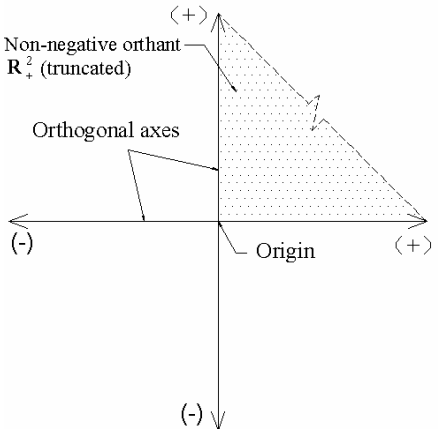

Fig. 1. Non-negative orthant R^2_+ (shaded and truncated).

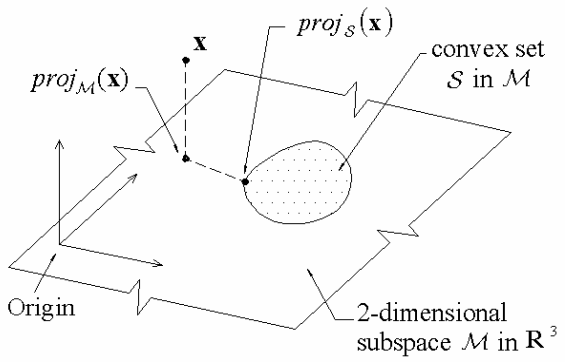

Fig 2. Projection onto a convex set in a subspace.

Euclidean-distance projection of a point $\mathbf{x}$ onto non-negative orthant R^n_+ can simply be obtained by zeroing all the negative entries of $\mathbf{x}$ as:

$$proj_{\mathrm{R}^n_+}(\mathbf{x}) = \max\{x_i, 0\} \quad \forall i \quad (i = 1, \ldots, n) \tag{5}$$

where $proj_{\mathrm{R}^n_+}(\mathbf{x})$ is the minimum-Euclidean-distance projection of $\mathbf{x}$ onto R^n_+.

III. Background on Static Analysis of CPM

For a spatial CPM the relationship between the cable tensions and the external load applied on the end-effector can be written as (Fig. 3):

$$\mathbf{w} = \begin{bmatrix} \mathbf{f} \\ \mathbf{m} \end{bmatrix} = -A\boldsymbol{\tau} \qquad (\tau_i \geq 0 \;\text{ for } i = 1, \ldots, n) \tag{6}$$

where $A = \begin{bmatrix} \mathbf{u}_1 & \cdots & \mathbf{u}_i & \cdots & \mathbf{u}_n \\ \mathbf{r}_1 \times \mathbf{u}_1 & \cdots & \mathbf{r}_i \times \mathbf{u}_i & \cdots & \mathbf{r}_n \times \mathbf{u}_n \end{bmatrix}$;

$\mathbf{f}$ and $\mathbf{m}$ are the external force and moment applied to the end-effector, respectively; n is the number of cables; $\boldsymbol{\tau}$ is an n-dimensional vector of the cable tensions; τ_i is the tension in the ith cable; $\mathbf{u}_i$ is a unit vector in the direction of the force applied by the ith cable to the mobile platform; and $\mathbf{r}_i$ is the position of the ith cable connection point on the mobile platform with respect to the end-effector.

To achieve static equilibrium against arbitrary external loads, CPM operating in an m-dimensional task space must satisfy the following conditions:

a) $n \geq m + 1$,

b) rank(A) = m, and

c) $\sum_{i=1}^{n} \begin{bmatrix} \alpha_i (\mathbf{u})_i \\ \beta_i (\mathbf{r})_i \times (\mathbf{u})_i \end{bmatrix} = \mathbf{0} \quad \alpha_i, \beta_i > 0$ (for $i = 1, \ldots, n$).

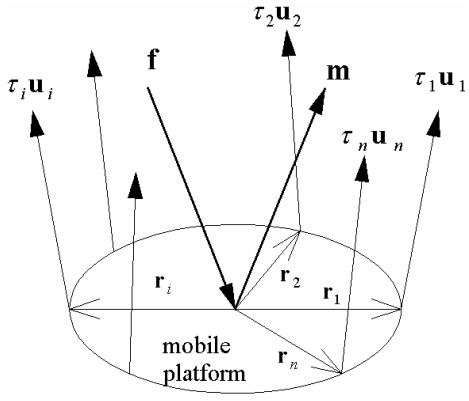

Fig. 3. Forces acting on mobile platform in CPM.

The above conditions are necessary for the existence of a solution for arbitrary external load $\mathbf{w}$. Assuming that these conditions are satisfied, there are infinitely many solutions for $\boldsymbol{\tau}$ because the manipulator becomes in this case redundantly actuated. In this study, a numerical technique is presented to resolve the actuation redundancy in (6) and determine the minimum norm solution for $\boldsymbol{\tau}$. This solution minimizes the overall actuator forces and, hence, minimizes the overall power consumption.

IV. Minimizing Overall Actuator Forces

In this section, a technique based on convex analysis is presented to determine the actuator force distribution that minimizes the 2-norm of the actuator forces in CPM for a given end-effector force and moment.

If the number of columns in matrix A in (6) is greater than its rank, then matrix A has a non-empty null space indicating that there are infinitely many solutions for $\boldsymbol{\tau}$. The general solution for $\boldsymbol{\tau}$ in (6) can be written as:

$$\boldsymbol{\tau} = -A^{+}\mathbf{w} + N\mathbf{h} \quad : \tau_i \geq 0 \quad \forall i \tag{7}$$

where A^{+} is the Moore-Penrose inverse, also known as the pseudo inverse, of matrix A; N is a matrix whose columns form a basis for the null-space of matrix A ; and $\mathbf{h}$ is a vector of arbitrary real numbers.

The solution in (7) consists of two parts: the first one is the term $-A^{+}\mathbf{w}$, which represents the minimum-norm solution that minimizes the 2-norm $\|\boldsymbol{\tau}\|$. The second part $N\mathbf{h}$ is an arbitrary vector in the null-space of matrix A and, hence, affects the distribution of the actuator forces without affecting the force and moment at the end-effector. Assuming that the manipulator is in a non-singular configuration and that there are no maximum limits placed on the cable tensions, a necessary condition for the existence of a solution is the existence of a null vector $N\mathbf{h}$ whose components are all positive [10]. The existence of this solution means that the cable-based parallel manipulator is fully constrained under any given end-effector force and moment, $\mathbf{f}$ and $\mathbf{m}$. Methods by which one can determine whether or not a cable-based manipulator is fully constrained at a given configuration can be found in [10] and [11]. In this study, it is assumed that the cable-based manipulator is fully constrained and it is required to determine the minimum-norm solution of $\boldsymbol{\tau}$ denoted as $\boldsymbol{\tau}_{\min\|\boldsymbol{\tau}\|}$. The condition that all components of $\boldsymbol{\tau}$ are non-negative means that $\boldsymbol{\tau}$ must belong to non-negative orthant R^n_+, i.e., $\boldsymbol{\tau} \in \mathrm{R}^n_+$, expressed as:

$$\mathrm{R}^n_+ = \left\{ \boldsymbol{\tau} \in \mathrm{R}^n \,\middle|\, \tau_i \geq 0 \;\; \forall i \right\} \tag{8}$$

By investigating (7), it is evident that the term $-A^{+}\mathbf{w} + N\mathbf{h}$ is an affine set, whose dimension is the same as that of the null space of A, in R^n. This affine set is formed by a subspace, whose basis is formed by the columns of matrix N, translated from the Origin ($\boldsymbol{\tau} = \mathbf{0}$) by $-A^{+}\mathbf{w}$. This affine set denoted here as $\mathcal{A}$ can be expressed as:

$$\mathcal{A} = \left\{ \boldsymbol{\tau} \,\middle|\, \boldsymbol{\tau} = -A^{+}\mathbf{w} + N\mathbf{h} \right\} \tag{9}$$

This affine set is basically a translation of the null space of matrix A from the Origin ($\boldsymbol{\tau} = 0$) by $-A^{+}\mathbf{w}$. Matrix N is a basis matrix of that null space. Since $\boldsymbol{\tau} \in \mathcal{A}$ and R^n_+, $\boldsymbol{\tau}$ belongs to the intersection of $\mathcal{A}$ and R^n_+, expressed as:

$$\boldsymbol{\tau} \in \mathcal{C} \quad : \mathcal{C} = \mathrm{R}^n_+ \bigcap \mathcal{A} \tag{10}$$

The minimum-norm solution for $\boldsymbol{\tau}$ in (7), $\boldsymbol{\tau}_{\min\|\boldsymbol{\tau}\|}$, is the unique minimum-Euclidean-distance projection of the Origin, $\boldsymbol{\tau} = \mathbf{0}$, onto convex set $\mathcal{C}$ (see Fig. 4). Hence, the solution can be expressed as:

$$\boldsymbol{\tau}_{\min\|\boldsymbol{\tau}\|} = proj_{\mathcal{C}}\left(\boldsymbol{\tau} = \mathbf{0}\right) \tag{11}$$

where $proj_{\mathcal{C}}\left(\boldsymbol{\tau} = \mathbf{0}\right)$ is the unique minimum-Euclidean-distance projection of the Origin onto $\mathcal{C}$.

As explained in Fig. 2, because $\mathcal{C} \subseteq \mathcal{A}$, $proj_{\mathcal{C}}\left(\boldsymbol{\tau} = \mathbf{0}\right)$ can be determined by projecting the Origin orthogonally onto $\mathcal{A}$ first and projecting the result onto $\mathcal{C}$ as:

$$\boldsymbol{\tau}_{\min\|\boldsymbol{\tau}\|} = proj_{\mathcal{C}}\left(\boldsymbol{\tau} = \mathbf{0}\right) = proj_{\mathcal{C}}\left(proj_{\mathcal{A}}\left(\boldsymbol{\tau} = \mathbf{0}\right)\right) \tag{12}$$

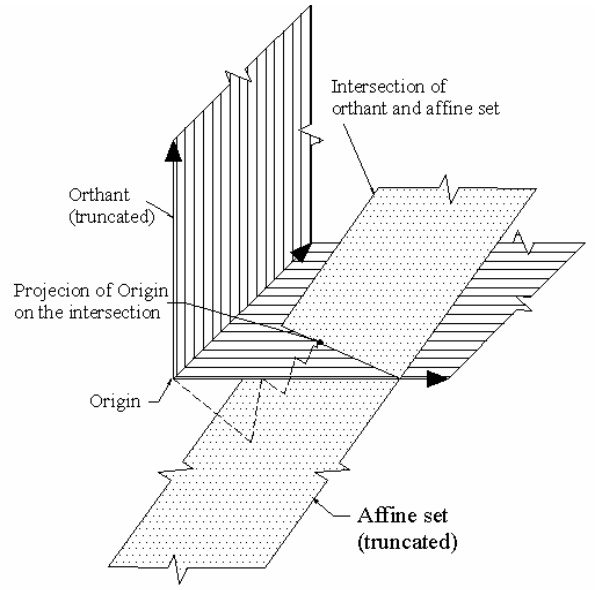

Fig. 4. An illustrative graph showing the projection of the Origin onto the intersection of an orthant with an affine set using alternating projections.

where $proj_{\mathcal{A}}(\boldsymbol{\tau}=\mathbf{0})$ is the minimum-Euclidean-distance projection of point $\boldsymbol{\tau}=\mathbf{0}$ onto $\mathcal{A}$; and $proj_{\mathcal{C}}\left(proj_{\mathcal{A}}(\boldsymbol{\tau}=\mathbf{0})\right)$ is the minimum-Euclidean-distance projection of $proj_{\mathcal{A}}(\boldsymbol{\tau}=\mathbf{0})$ onto $\mathcal{C}$. Because $proj_{\mathcal{A}}(\boldsymbol{\tau}=\mathbf{0})=-A^{+}\mathbf{w}$, (12) can be written as:

$$proj_{\mathcal{C}}(\boldsymbol{\tau}=\mathbf{0})=proj_{\mathcal{C}}\left(\boldsymbol{\tau}=-A^{+}\mathbf{w}\right) \tag{13}$$

Substituting (13) in (11):

$$\boldsymbol{\tau}_{\min\|\boldsymbol{\tau}\|}=proj_{\mathcal{C}}\left(\boldsymbol{\tau}=-A^{+}\mathbf{w}\right) \tag{14}$$

Since $\mathcal{C}$ is an intersection of two convex sets, an analytical solution for $proj_{\mathcal{C}}\left(\boldsymbol{\tau}=-A^{+}\mathbf{w}\right)$ cannot generally be determined. Instead, one can easily use the numerical alternating projection technique [14] to determine that solution. The alternating projection technique is an established iterative method that is based on projecting a point alternately on individual convex sets in order to reach to the minimum-Euclidean-distance projection of that point onto the intersection of those convex sets. Fig. 4 presents an illustration of the projection of a point onto the intersection of an orthant and an affine set. The *Dykstra*'s algorithm is a well-known alternating projection algorithm that was first presented by Dykstra [16] and reintroduced later by Han [17] who provided a proof of its convergence. This algorithm is used in this study to determine $proj_{\mathcal{C}}\left(\boldsymbol{\tau}=-A^{+}\mathbf{w}\right)$ in (14).

***The Dykstra's* algorithm**

To determine the minimum-Euclidean-distance projection of $\boldsymbol{\tau}=A^{+}\mathbf{w}$ onto the intersection set $\mathcal{C}$ of non-negative orthant R_{+}^{n} and affine set $\mathcal{A}$, let $\mathbf{x}_{k,i}$ and $\mathbf{y}_{k,i}$ belong to R^{n} where $\mathbf{x}_{k,i}$ is the minimum-Euclidean-distance projection of $\mathbf{t}\in\mathrm{R}^{n}$ onto convex set k at iteration i; and $\mathbf{y}_{k,i}=(\mathbf{x}_{k,i}-\mathbf{t})$. The algorithm initializes at i = 0, where $\mathbf{x}_{1,0}=-A^{+}\mathbf{w}$ is the initial point and $\mathbf{y}_{k,0}=0$ for all k.

for i = 1, 2, ..., until convergence
$\mathbf{x}_{1,i}=\mathbf{x}_{2,i-1}$
for k =1, 2 (where 1 and 2 are indices for R_{+}^{n} *and* $\mathcal{A}$*)*
$\mathbf{t}=\mathbf{x}_{k+1,i}-\mathbf{y}_{k,i-1}$
$\mathbf{x}_{k,i}=proj_{k}(\mathbf{t})$
$\mathbf{y}_{k,i}=(\mathbf{x}_{k,i}-\mathbf{t})$
loop end
loop end

This algorithm makes successive projections on $\mathcal{A}$ and R_{+}^{n} until it converges at the minimum-Euclidean-distance point from $\boldsymbol{\tau}=A^{+}\mathbf{w}$ to the intersection of $\mathcal{A}$ and R_{+}^{n}. Successive projections of $\mathbf{t}$ onto R_{+}^{n} and onto the affine set $\mathcal{A}$ are denoted, respectively, as $proj_{\mathrm{R}_{+}^{n}}(\mathbf{t})$ and $proj_{\mathcal{A}}(\mathbf{t})$. From (5), $proj_{\mathrm{R}_{+}^{n}}(\mathbf{t})$ is determined as:

$$proj_{\mathrm{R}_{+}^{n}}(\mathbf{t})=\max\{t_i,0\}\quad\forall i \tag{15}$$

Projection $proj_{\mathcal{A}}(\mathbf{t})$ can be determined as:

$$proj_{\mathcal{A}}(\mathbf{t})=\left(I-A^{+}A\right)\left(\mathbf{t}+A^{+}\mathbf{w}\right)-A^{+}\mathbf{w} \tag{16}$$

This projection basically represents projecting $\mathbf{t}$ onto the null space of A and translating the result by $-A^{+}\mathbf{w}$. The final solution $\boldsymbol{\tau}_{\min\|\boldsymbol{\tau}\|}$ is:

$$\boldsymbol{\tau}_{\min\|\boldsymbol{\tau}\|}=\mathbf{x}_{k,i}\quad:i=c \tag{17}$$

where c is the iteration i at which the algorithm converges, i.e., at which $\left\|\mathbf{x}_{k,c}-\mathbf{x}_{k,c-1}\right\|+\left\|\mathbf{y}_{k,c}-\mathbf{y}_{k,c-1}\right\|\le\varepsilon$.

This solution minimizes the overall actuator forces, and, hence, minimizes the power consumption at a given end-effector loading.

V. EXAMPLES

In the following, the procedure explained in this paper is applied to a 3-DOF and a 6-DOF spatial cable-based parallel

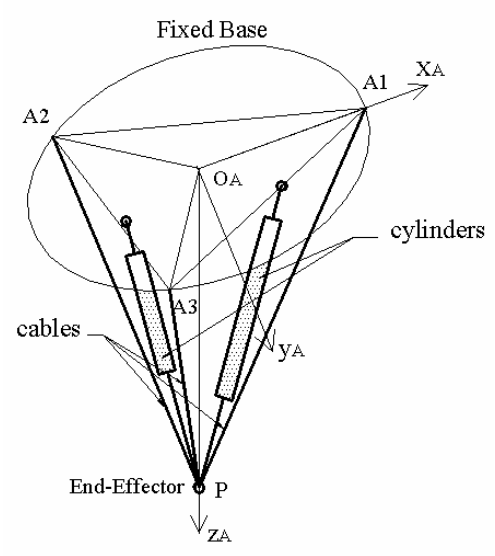

Fig. 5. A schematic diagram of the 3-DOF example manipulator.

manipulators (CPM).

A. 3-DOF Spatial CPM

As shown in Fig. 5, the layout of this manipulator consists of three cables and two redundant limbs (cylinders) whose role is to keep the cables in tension. These two cylinders only apply forces in one direction and, therefore, can be modeled as redundant cables. They meet at point P, which is the end-effector point in a translation-only task space. The three cables are connected to the fixed base on the top at points A_i (i = 1, 2, 3) that form an equilateral triangle, where subscript i is an index identifying each cable. The corners of the triangle lie on a circle with a 300 mm radius with its centre located at O_A. The coordinate frame x_A-y_A-z_A is attached to the fixed base at point O_A with the x_A-axis passing through point A_1. Redundant limbs (cylinders) 1 and 2 are connected to the base at [129.9 75.0 0] mm and [−129.9 75.0 0] mm, respectively. The position of P (end-effector) is [0 0 300] mm from O_A. The external force applied to the end-effector is $\mathbf{w} = [-10\ -7\ -10]^T$ N. It is required here to determine the minimum-norm solution $\boldsymbol{\tau}_{\min\|\boldsymbol{\tau}\|}$. At this configuration, matrix A is calculated as:

$$A = -\begin{bmatrix} 0.707 & -0.354 & -0.354 & -0.387 & 0.387 \\ 0 & -0.612 & 0.612 & -0.224 & -0.224 \\ -0.707 & -0.707 & -0.707 & 0.894 & 0.894 \end{bmatrix}$$

The first three columns are the directions of the cables forces and the last two columns are the directions of the redundant-limb forces. These redundant limbs are cylinders that apply compressive-only forces to the mobile platform. The term $-A^{+}\mathbf{w}$ in (7) is calculated as $[3.51\ -12.95\ -0.24\ -1.93\ 5.45]^T$ N. The *Dykstra's* alternating projection algorithm is applied to determine the minimum-Euclidean-distance projection of $-A^{+}\mathbf{w}$ onto the intersection of non-negative orthant R^5_+ and affine set $\mathcal{A}$ in (9), using the projection formulas in (15) and (16). Table I lists the projections onto R^5_+ and $\mathcal{A}$ until it converges to the minimum-norm solution, which is $\boldsymbol{\tau}_{\min\|\boldsymbol{\tau}\|} = [6.74\ 0.00\ 0.00\ 24.54\ 35.91]^T$ N with $\varepsilon \le 1^{-2}$. Each row of this table represents a cycle of projections which consists of two projections, one onto R^5_+ and another onto $\mathcal{A}$. The norm $\left\|\boldsymbol{\tau}_{\min\|\boldsymbol{\tau}\|}\right\| = 44.02$ is the minimum norm for $\boldsymbol{\tau}$ at the given external load $\mathbf{w}$. The terms $\boldsymbol{\tau}_{c1}, \ldots, \boldsymbol{\tau}_{c3}$ are the forces along the three cables while $\boldsymbol{\tau}_{r1}$ and $\boldsymbol{\tau}_{r2}$ are the forces of the two redundant limbs (cylinders).

TABLE I
ALTERNATING-PROJECTION RESULTS FOR THE 3-DOF EXAMPLE

Iter-ation	Projections on R^5_+					Projections on $\mathcal{A}$				
	$\boldsymbol{\tau}_{c1}$	$\boldsymbol{\tau}_{c2}$	$\boldsymbol{\tau}_{c3}$	$\boldsymbol{\tau}_{r1}$	$\boldsymbol{\tau}_{r2}$	$\boldsymbol{\tau}_{c1}$	$\boldsymbol{\tau}_{c2}$	$\boldsymbol{\tau}_{c3}$	$\boldsymbol{\tau}_{r1}$	$\boldsymbol{\tau}_{r2}$
1	3.51	0.00	0.00	0.00	5.45	4.36	-11.66	2.45	-1.05	8.39
2	4.36	0.00	2.24	0.00	8.39	4.76	-10.57	4.60	-0.72	10.95
3	4.76	0.00	4.60	0.00	10.95	5.05	-9.53	6.59	-0.53	13.38
4	5.05	0.00	6.59	0.00	13.38	5.26	-8.59	8.37	-0.43	15.59
5	5.26	0.00	8.37	0.00	15.59	5.42	-7.75	9.97	-0.36	17.59
77	6.74	0.00	24.54	0.00	35.90	6.74	0.00	24.54	0.00	35.91
78	6.74	0.00	24.54	0.00	35.91	6.74	0.00	24.54	0.00	35.91
79	6.74	0.00	24.54	0.00	35.91	6.74	0.00	24.54	0.00	35.91

B. 6-DOF Spatial CPM

As shown in Fig. 6, this manipulator consists of six cables and three redundant limbs (cylinders) connecting the base to the mobile platform. Similarly, these cylinders only apply forces in one direction and, therefore, can be modeled as redundant cables. Points A_i and B_i form an equilateral triangle in the mobile platform and lie on a 200-mm-radius circle whose centre is O_B, where subscript i identifies each cable. The coordinate frames x_A-y_A-z_A and x_B-y_B-z_B are attached to the fixed base and mobile platform, respectively. The three redundant limbs are connected to the base at points located at [210.0 0.0 0.0] mm, [−105.0 −181.9 0.0] mm, and [−105.0 181.9 0.0] mm from O_A. The connections of the three redundant limbs to the mobile platform are respectively [100.0 0.0 0.0] mm, [−50.0 −86.6 0.0] mm, and [−50.0 86.6 0.0] mm respectively, from O_B. The mobile platform has a zero orientation relative to the base and point O_B is located at [0.0 0.0 300.0] mm from O_A. The external force and moment applied to the end-effector is $\mathbf{w} = [\,\mathbf{f}^T\ \mathbf{m}^T\,]^T$ where $\mathbf{f} = [-10\ 5\ -10]^T$ N applied to point O_B and $\mathbf{m} = [8\ -5\ 3]^T$ Nm both expressed in x_A-y_A-z_A coordinate frame. The inverse kinematics solution for this manipulator can be found in [18]. The term $-A^{+}\mathbf{w}$ in (7) is calculated as $[0.73\ -4.63\ 1.66\ -2.69\ -6.15\ 3.59\ -0.82\ 1.73\ 3.77]^T$ N, where the first six components correspond to the cables while the last three columns correspond to the three redundant limbs.

Similarly, to determine the minimum-norm solution, the

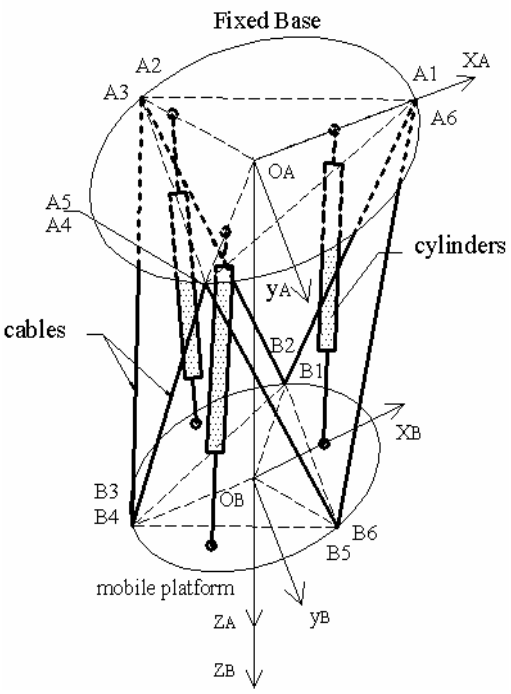

Fig. 6. A schematic diagram of the 3-DOF example manipulator.

Dykstra's alternating projection algorithm is applied to find the minimum-Euclidean-distance projection of $A^{+}\mathbf{w}$ onto the intersection of non-negative orthant R_{+}^{9} and affine set $\mathcal{A}$. The results of the successive projections are listed in Table II and the final solution is $\boldsymbol{\tau}_{\min\|\boldsymbol{\tau}\|}$= [3.70 0.00 7.23 4.01 0.00 6.94 3.04 10.01 15.08]^{T} N with $\varepsilon \le 1^{-3}$. The terms $\boldsymbol{\tau}_{c1},\ldots,\ \boldsymbol{\tau}_{c6}$ are the forces along the six cables while $\boldsymbol{\tau}_{r1}$ and $\boldsymbol{\tau}_{r3}$ are the forces of the three redundant limbs (cylinders).

VI. Conclusion

It is seen that convex analysis provided an efficient way to formulate the static analysis of cable-based parallel manipulator addressing the constraints imposed on the cable forces. In this study, a numerical approach based on alternating projection was presented to find the minimum-norm solution for the forces in the cables and the redundant limbs. The alternating projection algorithm was applied on two different example manipulators. The minimum-norm solution minimizes the overall actuator forces and, hence, minimizes the power consumption during the operation.

References

[1] S. Kawamura, and K. Ito, "A New Type of Master Robot for Teleoperation Using a Radial Wire Drive System", in *Proc. 1993 IEEE Int. Conf. Intell. Robots and Systems*, pp. 55-60.

[2] A. Ming, and T. Higuchi, "Study on Multiple Degree-of-Freedom Positioning Mechanism Using Wires (Part 1)", *Int. J. Japan Society of Precision Engineering*, vol. 28, no. 2, pp. 131-138, 1994.

[3] A. Russell, "A Robotic System for Performing Sub-millimeter Grasping and Manipulation Tasks", *Robotics and Autonomous Systems*, vol. 13, pp. 209-218, 1994.

[4] S. Behzadipour, and A. Khajepour, "A New Cable-based Parallel Robot with Three Degrees of Freedom", *Multibody System Dynamics*, vol. 13, pp. 371-383, 2005.

[5] J. Albus, R. Bostelman, and N. Dagalakis, "The Nist Robocrane", *J. Robotic Systems*, vol. 10, no. 5, pp. 709-724, 1993.

[6] S. Kawamura, W. Choe, and S. Tanak, "Development of an Ultrahigh Speed Robot Falcon Using Wire Driven Systems", in *Proc. 1995 IEEE Int. Conf. on Robot. Autom.*, pp. 215-220.

[7] K. Maeda, S. Tadokoro, T. Takamori, M. Hiller, and R. Verhoeven, "On Design of a Redundant Wire-driven Parallel Robot WARP Manipulator" in *Proc. 1999 IEEE Int. Conf. on Robot. Autom.*, vol. 2, pp. 895-900.

[8] C. Ferraresi, M. Paoloni, and F. Pescarmona, "A new 6-dof Parallel Robotic Structure Actuated by Wires: The Wiro-6.3", *J. of Robotic Systems*, vol. 21, no. 11, pp. 581-595, 2004.

[9] G. Mroz, and L. Notash, "Wire-actuated Robots with a Constraining Linkage", *J. Robotic Systems*, vol. 21, no. 12, pp. 677-678, 2004.

[10] R. G. Roberts, T. Graham, and T. Lippitt, "On the Inverse Kinematics, Statics, and Fault Tolerance of Cable-Suspended Robots", *J. Robotic Systems*, vol. 15, no. 10, pp. 581-597, 1998.

[11] E. Stump, and V. Kumar, "Workspaces of Cable-Actuated Parallel Manipulators", *ASME J. Mechanical Design*, vol. 128. no. 1, pp. 159-167, 2006.

[12] M. Hassan, and A. Khajepour, "Optimum Connection Positions for the Redundant Limb in Cable-based Parallel Manipulators", *ASME International Mechanical Engineering Congress and Exposition (IMECE)*, Chicago, Illinois, U.S.A., November 2006.

[13] S. Fang, D. Franitza, M. Torlo, F. Bekes, and M. Hiller, "Motion Control of a Tendon-Based Parallel Manipulator Using Optimal Tension Distribution", *IEEE/ASME Trans. Mechatronics*, vol. 9, no. 3, pp. 561-568, 2004.

[14] J. Dattorro, *Convex Optimization & Euclidean Distance Geometry*, Meboo Publishing, U.S.A., 2005.

[15] S. Behzadipour, *Ultra-high-speed Cable-based Robots*, Ph.D. Thesis, Dept. Mech. Eng., University of Waterloo, Waterloo, Ontario, Canada, 2005.

[16] R. L., Dykstra, "An Algorithm for Restricted Least Squares Regression", *Journal of the American Statistical Association*, vol. 87, no. 384, pp. 837-842, 1983.

[17] S.-P. Han, "A successive projection method", *Mathematical Programming*, vol. 40, pp.1-14, 1988.

[18] L. W. Tsai, Robot Analysis: *The Mechanics of Serial and Parallel Manipulators*, Wiley-Interscience Publication, 1999.

TABLE II
ALTERNATING-PROJECTION RESULTS FOR THE 6-DOF EXAMPLE

Iter-ation	Projections on R_{+}^{9}									Projections on $\mathcal{A}$								
	$\boldsymbol{\tau}_{c1}$	$\boldsymbol{\tau}_{c2}$	$\boldsymbol{\tau}_{c3}$	$\boldsymbol{\tau}_{c4}$	$\boldsymbol{\tau}_{c5}$	$\boldsymbol{\tau}_{c6}$	$\boldsymbol{\tau}_{r1}$	$\boldsymbol{\tau}_{r2}$	$\boldsymbol{\tau}_{r3}$	$\boldsymbol{\tau}_{c1}$	$\boldsymbol{\tau}_{c2}$	$\boldsymbol{\tau}_{c3}$	$\boldsymbol{\tau}_{c4}$	$\boldsymbol{\tau}_{c5}$	$\boldsymbol{\tau}_{c6}$	$\boldsymbol{\tau}_{r1}$	$\boldsymbol{\tau}_{r2}$	$\boldsymbol{\tau}_{r3}$
1	0.74	0.00	1.66	0.00	0.00	3.59	0.00	1.73	3.77	1.45	-3.78	2.71	-1.17	-4.67	4.47	0.26	3.15	6.45
2	1.45	0.00	2.71	0.00	0.00	4.47	0.00	3.15	6.45	1.74	-3.16	3.52	-0.13	-3.74	4.83	0.54	4.32	8.24
3	1.74	0.00	3.52	0.00	0.00	4.83	0.00	4.32	8.24	1.88	-2.69	4.14	0.58	-3.14	5.00	0.58	5.26	9.42
42	3.70	0.00	7.22	4.01	0.00	6.94	3.04	10.01	15.08	3.70	0.00	7.23	4.01	0.00	6.94	3.04	10.01	15.08
43	3.70	0.00	7.23	4.01	0.00	6.94	3.04	10.01	15.08	3.70	0.00	7.23	4.01	0.00	6.94	3.04	10.01	15.08
44	3.70	0.00	7.23	4.01	0.00	6.94	3.04	10.01	15.08	3.70	0.00	7.23	4.01	0.00	6.94	3.04	10.01	15.08